Electron temperature fluctuation levels of the quasi-coherent mode across the plasma radius

Branka Vanovac[1,*], *Jörg* Stober[2], *Elisabeth* Wolfrum[2], *Matthias* Willensdorfer[2], *Luís* Gil[3], *Michael* Faitsch[2], *Rachel* Bielajew[1], *Christian* Yoo[1], *Garrard* Conway[2], *Severin* Denk[1], *Rachael* McDermott[2], *Anne* White[1], and *ASDEX* Upgrade Team[4]

[1]Massachusetts Institute of Technology, Plasma Science and Fusion Center, Cambridge, MA 02139, USA
[2]Max Plank Institute for Plasma Physics, 85748 Garching, Germany
[3]Instituto de Plasmas e Fusão Nuclear, Instituto Superior Técnico, Universidade de Lisboa, 1049-001 Lisboa, Portugal
[4]See author list of U. Stroth et al. 2022 Nucl. Fusion 62 042006

Abstract. EDA H-mode is an ELM-free regime in which the edge quasi-coherent mode (QCM) replaces the ELMs. The estimated location of the quasi-coherent mode is in a partly optically thin region of steep gradients localized between ρ_{pol} = 0.96 -1. Relative fluctuations of radiation temperature between 15 and 80 kHz are about 7% with significant density contribution. In the electron cyclotron emission (ECE) channels with resonances in the plasma core, a mode with the same frequency as the quasi-coherent mode is measured. The peak amplitude of both core and edge modes matches the strongest electron temperature gradient in the core and the edge, respectively. The ECE core and edge signals are out of phase. The radiation transport forward model (ECRad) shows that the refraction explains the phase relation between the edge and the core ECE channels. The phase correlates with the sign of the core ∇T_e. The amplitude of the fluctuations in the core decreases with decreasing gradients, which is the trend seen in the experiment. The amplitude ratio of the core and edge fluctuation is a factor of five in the experiment; this ratio remains a factor of a hundred in the modeling.

1 Introduction

The EDA H-mode (Enhanced D_α high confinement mode) regime is a regime free of edge localized modes (ELMs) with good energy confinement properties [1]. Recently it has been a significant focus of the ASDEX Upgrade experimental program and its main features are reported in [2]. At ASDEX Upgrade, the dominant external heating is the electron cyclotron resonance heating (ECRH) and the rotation profiles are hollow, similar to observations in some L-mode plasmas [3]. The ELMs are replaced by a quasi-coherent mode thought to regulate the transport and keep the pedestal stable against large type-I ELMs. The EDA H-mode regime is routinely obtained at ASDEX upgrade and the neutral beam injection NBI power window is extended with Ar seeding [4]. As mentioned, the prominent signature of EDA H-mode is the quasi-coherent mode measured at the plasma edge with different diagnostics; thermal He-beam emission spectroscopy (THB), electron cyclotron emission (ECE), and reflectometers. However, in some core ECE channels, a fluctuation appears with the same frequency as the quasi-coherent mode and is absent in the signals of other core diagnostics i.e., soft X-rays. The origins of the core ECE emission have been debated, and the main question remains whether it is a consequence of the strong refraction on the edge density or actual core fluctuations.

*e-mail: vanovac@mit.edu

The quasi-coherent mode (QCM) in the plasma edge is a feature of the EDA ELM-free regime, but it can also coexist with ELMs in ELMy H-modes, most likely appearing between ELMs. However, in the context of this work, we will refer only to the quasi-coherent mode where ELMs are absent and describe it in terms of its frequency and associated temperature fluctuation amplitudes.

The relative temperature fluctuation levels across the pedestal are assessed via the Correlation Electron Cyclotron Emission (CECE) instrument [5] covering the region of $\rho_{pol} = [0.85 - 1]$ while the standard ECE diagnostics is used for core-edge amplitude comparison and comparison to the modeling. EC Radiation transport is assessed with ECRad [6], a radiation transport code suitable for treating electron cyclotron emission with specifics of CECE and ECE diagnostics such as launching angles and IF bandwidth. Refraction is included in ECRad, allowing studies on the refractive effects on the core emission.

2 Features of quasi-coherent mode

2.1 Frequency

The peak frequency of the quasi-coherent mode at ASDEX Upgrade during its stationary phase varies between 15 and 60 kHz. The calculated power spectral density from the ECE measurements at three different radial locations is displayed in figure 1. The peak frequency is determined

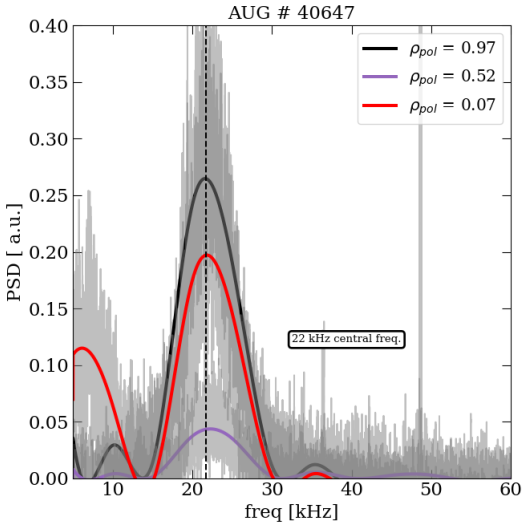

Figure 1. AUG #40647: Power spectral density of ECE measurements at three different locations as indicated by different colors $\rho_{\mathrm{pol}} = 0.97$ in black, $\rho_{\mathrm{pol}} = 0.52$ in purple and $\rho_{\mathrm{pol}} = 0.07$ in red. The black dashed line marks the center frequency of about 22 kHz.

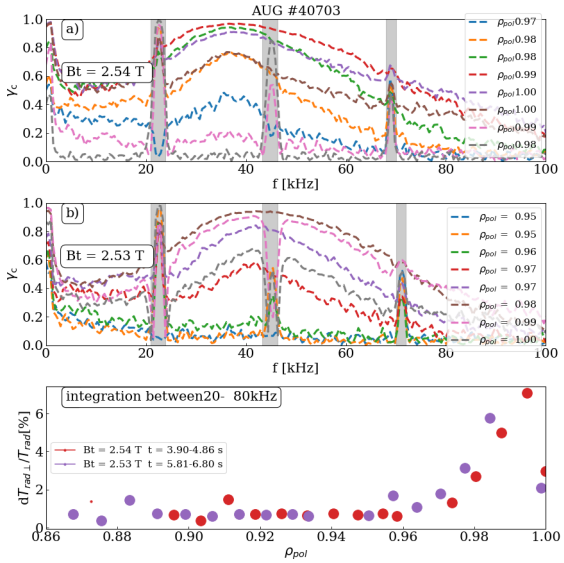

Figure 2. AUG #40703 a) Cross-coherence between subsequent CECE channels for magnetic field strength of 2.54 T. b) Cross-coherence between subsequent correlation ECE channels for magnetic field strength of 2.53 T. c) Relative radiation temperature fluctuations integrated between 20 and 80 kHz from the CECE measurements for $B_t = 2.54$ T in red and for $B_t = 2.53$ T in magenta, respectively. Grey regions are marking peaks of strong noise in the channels.

from the spline fit to the data shown in gray. The black curve shows the power spectrum measured at the edge at $\rho_{\mathrm{pol}} = 0.97$, the purple one at $\rho_{\mathrm{pol}} = 0.52$ at the mid-radius, while the red curve corresponds to the measurement in the plasma core at $\rho_{\mathrm{pol}} = 0.07$. The peak frequency for both the edge and the core is identical at f = 22 kHz, indicating the same feature measured in both plasma regions. The power spectra broaden due to the changes in the frequency of the quasi-coherent mode during the integration time.

2.2 Localisation and amplitude

We use the CECE system for the localization and δT_{rad} estimate. The CECE system at ASDEX Upgrade is a comb of 24 channels with fixed IF filters of 200 MHz bandwidth and 250 MHz spacing of the center frequencies, translating into approximately 2 mm of spatial resolution. Neighboring CECE channels measure correlated temperature fluctuations but uncorrelated thermal noise. By correlating neighbouring channels, coherency spectra γ_c of turbulence are obtained. We obtain the fluctuation amplitude by integrating coherency in frequency space and subtracting the background noise. A dedicated experiment with two magnetic field strengths enables more accurate localization of the QCM. With changing magnetic field strength, the measurement position of the ECE & CECE channels changes while the mode location remains the same. Consequently, the mode amplitude moves from one channel to the next. In figure 2 we show the CECE measurements during discharge #40703, for both field strengths. Figure 2 a) and 2 b) show the coherency spectra γ_c against normalized radius. Figure 2 c) displays the relative temperature fluctuation levels versus normalized plasma radius ρ_{pol} for Bt = 2.54 T in red and for Bt = 2.53 T in magenta. The mode affects the radial range between $\rho_{\mathrm{pol}} = 0.96$ and the separatrix in both cases. Due to the low optical depth outside of $\rho_{\mathrm{pol}} = 0.97$, the fluctuation amplitudes of 7% can be a consequence of density perturbation in this region [7].
Profile ECE measurements integrated between 15 and 60 kHz are shown in figure 3 for the same discharge #40703. Corresponding temperature profiles are shown in 3 a) and profile gradients in 3 b). For both magnetic field strengths, the maximum amplitude distribution (shown in 3 c)) matches the peak of the electron temperature gradients in the edge and the core of the plasma.

A typical feature of EDA H-mode is the high electron density, however, in our experiment ECE radiation is always below the cutoff and the ECE profile measurements are routinely obtained. The electron temperature and density profiles for two cases comparing two discharges are shown in figure 4. The discharge #40647 had plasma current $I_p = 0.6$ MA while the discharge #40417 had $I_p = 0.7$ MA and consequently higher density. Both discharges had the same magnetic field strength and the ECRH heating scheme. The higher current discharge had NBI blips applied for charge exchange measurements.

The corresponding temperature fluctuations across the pedestal for both cases averaged over 2 s of the discharges are shown in figure 5. The behavior of the radiation temperature fluctuations for two different density profiles differs. The T_{rad} fluctuations for the low pedestal density case are increasing from 0.97 and peak just before the separatrix. The T_{rad} fluctuations for the high pedestal density case are increased across an entire measurement region. This major difference in the shape of the radial ampli-

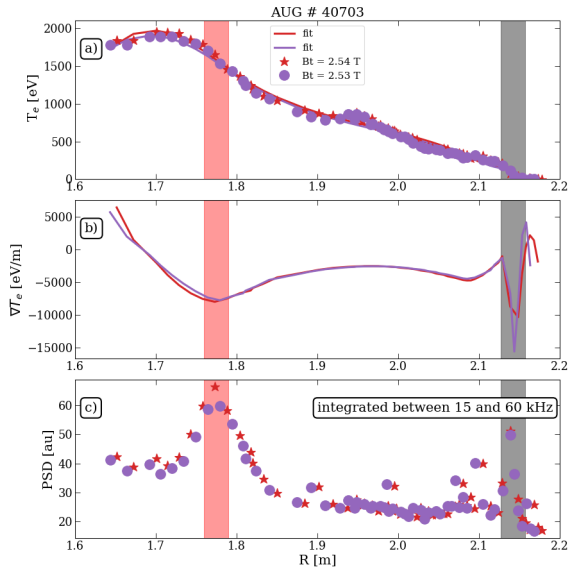

Figure 3. AUG # 40703 with changing magnetic field; 2.53 T in magenta and 2.54 T in red a) The electron temperature profiles, b) the gradient of the electron temperature, c) amplitude distribution integrated between 15 and 60 kHz corresponding to the quasi-coherent mode

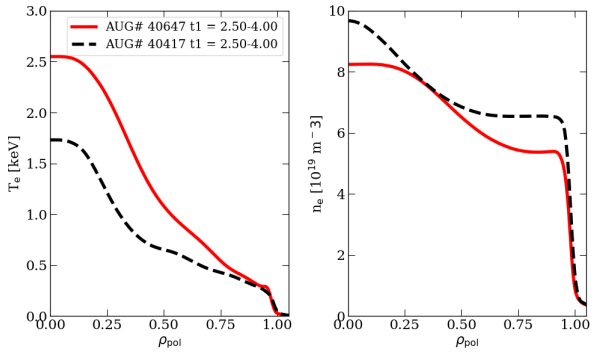

Figure 4. Profiles obtained with integrated data analysis (IDA) for low AUG # 40647 and high AUG # 40417 pedestal density discharges averaged during time interval t = 2.5 - 4 s. Low pedestal density is displayed in red while high pedestal density case is shown in black.

tude distribution of the temperature fluctuations suggests its density dependence.

2.3 Changing core T_e gradients

Figure 6 displays an EDA H-mode designed to study the effect of core temperature gradient on the quasi-coherent activity measured in the core and edge ECE channels. The temperature gradient during the discharge was changed by the ECRH deposition shifting from central to off-axis heating. The discharge has a plasma current of I_p = 600 kA and a magnetic field B_T = 2.5 T. Figure 6 a) illustrates the ECRH heating scheme. Between 2-4 s two central gyrotrons heat the plasma. The second phase, between 4-6 s combines one central gyrotron and one mid-radius

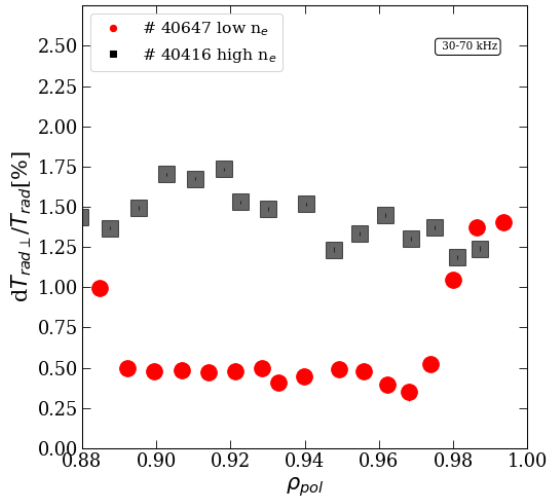

Figure 5. Radial profiles of the relative radiation temperature fluctuations measured by the correlation ECE instrument for two different density values; low pedestal density # 40647 in red and high pedestal density # 40417 in black.

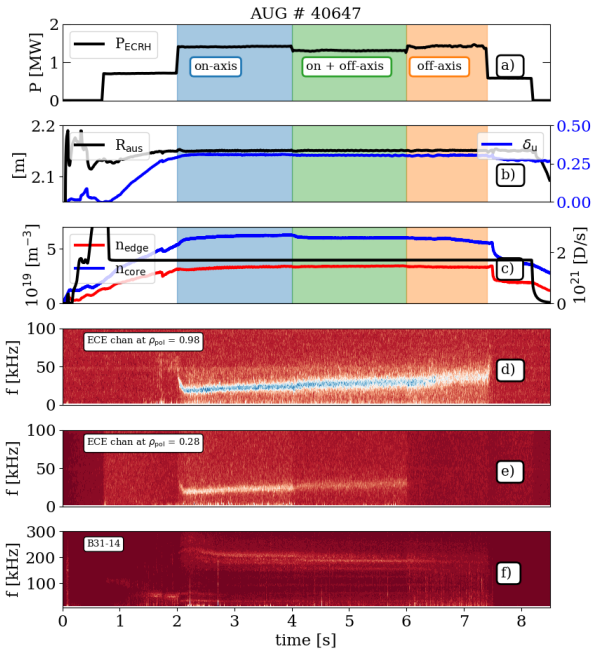

Figure 6. AUG # 40647: Temporal evolution of plasma parameters during EDA H-mode. a) ECRH heating scheme. b) Outer plasma boundary R_{aus} (black) and upper triangularity δ_u (blue). c) edge and core densities together with the deuterium fuelling. d) Spectrogram of the edge ECE channel. e) Spectrogram of the ECE core channel. f) Spectrogram of the magnetic coil B31-14 measuring changes in the radial magnetic field. Time intervals of different heating schemes are marked in colored surfaces: blue - on-axis heating; green - on and off-axis heating; orange - off-axis heating.

gyrotron. In the last phase, between 6-7.4 s, both gyrotrons deposit the power at mid-radius. The total power is about 1.4 MW throughout the discharge. The plasma had a fixed shape as represented by the upper triangularity δ_u

and the outer plasma boundary R_{aus} as displayed in figure 6 b). The core and edge densities as well as the fueling are shown in figure 6 c) and remained constant throughout the discharge. Spectrograms of the edge and core ECE channels, displayed in figure 6 d) and 6 e) show the quasi-coherent mode. Figure 6 f) displays the spectrogram of the magnetic coil measuring radial magnetic field fluctuations at the outer midplane. The strongest modes in the coil are around 200 kHz frequency, usually with toroidal mode numbers n = 5,6 and 7. The fundamental frequency of this harmonic structure has a frequency similar to the quasi-coherent mode in this example. The profile comparison between on and off-axis ECRH heating during the discharge # 40647 is displayed in figure 7. The phase with on-axis heating is marked in blue, and the phase with off-axis heating is in orange. The average profiles measured with ECE are displayed as symbols, and corresponding fits as lines in figure 7 a). The estimated gradients of the measured and fitted profiles are shown in 7 b). The radial distribution of the ECE amplitude measurement integrated between 15 and 60 kHz is displayed in 7 c). The location of the peak amplitude and matching gradients is emphasized with a shaded region the core being in red and the edge marked in black.

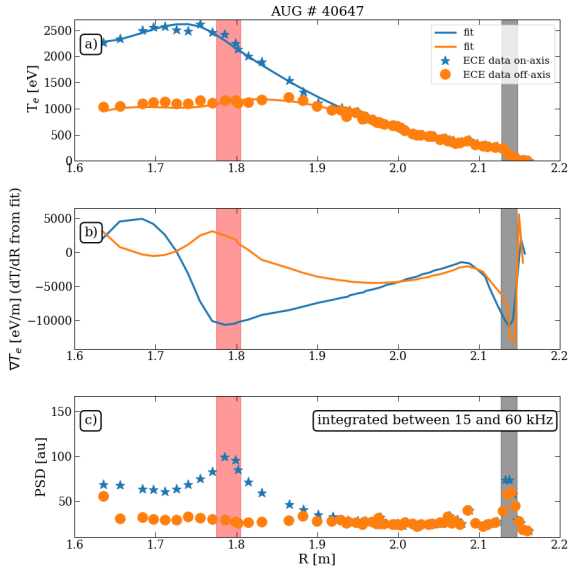

Figure 7. AUG # 40647 profiles for the two different heating schemes. On-axis ECRH heating is shown in blue while off-axis is shown in orange. a) Profile of the electron temperature T_e measured with ECE in symbols and the corresponding fits in solid lines. b) Gradients of the electron temperature fits. c) Amplitude distribution of Fourier filtered data between 15 and 60 kHz. The two shaded regions correspond to the maximum perturbation amplitude in the core (in red) and at the edge (in black).

3 Refraction effects

The edge quasi-coherent mode is the primary candidate for particle transport across the pedestal. However, the measurements of the quasi-coherent mode in the core ECE channels remain ambiguous. One hypothesis is that the mode measured in the core ECE channels is due to the refraction of the beams on a high-density perturbation at the edge. Another important ingredient is the steepness of the temperature profile.

Density fluctuations are measured with a thermal He beam and reflectometers. Another supporting argument is the absence of the core mode in other core diagnostics, i.e. soft X-ray measurements. To account for the possible refraction from the significant density perturbation at the edge, we employ the radiation transport forward model ECRad [6] where the geometry of the ECE system is included. We model the steep and the flat temperature profile scenarios of the discharge shown in figure 7. In the modeling we use a single ray, hence the observation volume is neglected. As input to the ECRad we use a two-dimensional T_e and n_e grid. Raytracing is then performed and the radiation transport equation is solved along the ray path for each time-point, resulting in time-resolved radiation temperature. The 2D data used for the modeling is the output of a recent JOREK simulation for a regime with small ELMs [8] regime, where a rotating mode at 20 kHz with n = 10 was observed. This set of data is, at present, suitable to treat the quasi-coherent mode as the perturbation structure of the small ELMs scenario has similar features as the quasi-coherent mode in terms of frequency, toroidal mode number and the extent across the pedestal. The JOREK simulation is performed for a different discharge than the one treated in this work. Therefore, JOREK data is further modified to be closer to the shape and magnitude of the background electron density and temperature profiles of the discharge # 40647.

The final modified profiles are fed separately into ECRad for the two cases. The modeling is performed for fifteen-time points to obtain time-resolved radiation temperatures. We then calculate the relative radiation temperature fluctuations $(T_{rad} - \langle T_{rad} \rangle)/\langle T_{rad} \rangle$ for each time point where $\langle T_{rad} \rangle$ is an equilibrium temperature without perturbation. The result for the case of the steep electron temperature profile is displayed in figure 8. We compare two different radial locations. The core channel is at $\rho_{pol} = 0.21$ shown in red and the edge ECE channel at $\rho_{pol} = 0.98$ in black. The edge and the core fluctuations are in anti-

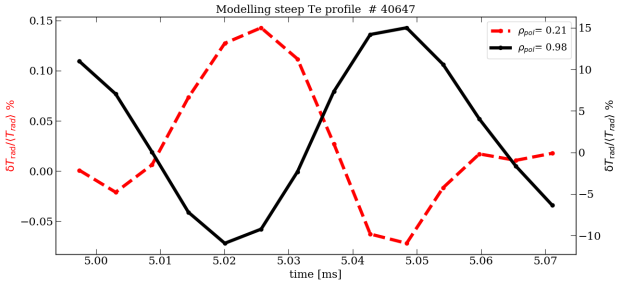

Figure 8. ECRad modeling: modelled time evolution of the radiation temperature fluctuations for the on-axis heating case. Black solid line shows the channel at the plasma edge while red dashed line represents the behaviour in the core.

phase. The maximum amplitude of the core channel is about 0.15 %, while the radiation temperature fluctuations at the edge are 15 %, making it a factor of 100 difference between the edge and the core, in this modeling exercise.

Now we compare this modeling result to the experimental measurements. The time-resolved ECE measurements (experiment) in the core and the edge of the plasma, for the on-axis heating scenario, are shown in figure 9. The channel at $\rho_{\mathrm{pol}} = 0.2$ is displayed in red while the edge channel at $\rho_{\mathrm{pol}} = 0.98$ is shown in black. The phase relation between the edge and the core changes over time. However, for the majority of the time, the two signals are close to anti-phase, similar to the modeling (see figure 8). Core and edge amplitude differ by a factor of 5.

A modeling is then performed for the case with an off-axis

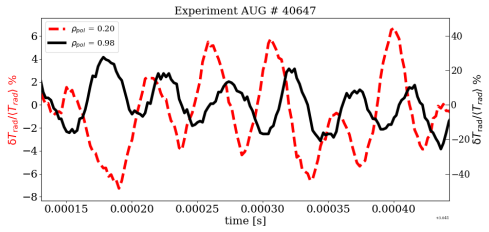

Figure 9. AUG # 40647: time evolution of the $\delta T_e/\langle Te\rangle$ obtained from the raw ECE data in the core $\rho_{\mathrm{pol}} = 0.2$ (red) and at the edge at $\rho_{\mathrm{pol}} = 0.98$ (black).

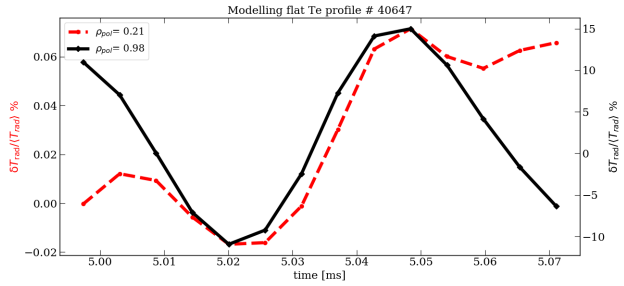

Figure 10. ECRad modeling: modelled time evolution of the radiation temperature fluctuations for the off-axis heating case. Black solid line shows the channel at the plasma edge while red dashed line represents the behaviour in the core.

ECRH heating scheme in which case the flat core temperature profile is flat. A comparison between relative temperature fluctuations of the two different radial locations for the off-axis scenario is shown in figure 10. The core channel is at $\rho_{\mathrm{pol}} = 0.21$ in red and the edge ECE channel at $\rho_{\mathrm{pol}} = 0.98$ in black. The amplitude of the core fluctuation is about 0.06 %, which is 2.5 times smaller than in the case of the steep gradient. The edge fluctuation amplitude remains unchanged, which is expected since the only change to the modeling input is the temperature profile in the plasma core. The core and the edge channels are in phase. This is a consequence of the sign of the temperature gradient. In the case of the flat ∇T_e, the core temperature leans towards the hollow core profile, allowing for the temperature gradient of the opposite sign if compared to the steep gradient case. This comparison is best seen in figure 7b).

For better clarity, figure 11 shows the ray path of one of the core ECE frequencies. The equilibrium ray path without perturbation is shown in black, while the red corresponds to the ray path with edge perturbation included. Corresponding resonances are marked with squared symbols. The bending of the ray path happens at the edge, which is seen in the zoomed edge region. As a consequence, the resonances are vertically displaced in the core.

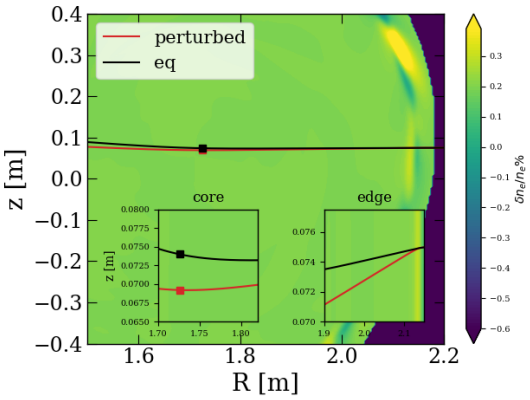

Figure 11. 2D density contour plot with density perturbation at the edge used in the forward model. The ECE ray is refracted at the edge which can be seen in the zoomed picture and the resonance (in red) is displaced with respect to the equilibrium (black) position.

4 Conclusion and Outlook

The correlation ECE instrument makes it possible to obtain the relative temperature fluctuation levels of the quasi-coherent mode at the plasma edge. Estimated fluctuation T_{rad} levels integrated between 20-80 kHz are around 7%. The location of the quasi-coherent mode is measured to be in the region of steep gradients between $\rho_{\mathrm{pol}} = 0.96$ -1 of insufficient optical depth, where density contributes to the measured radiation temperature fluctuations. Two scenarios with different plasma currents show differences in the trends when comparing the relative temperature fluctuations estimated with the correlation ECE instrument. With higher density, the fluctuations amplitude pattern seems to be flat across the gradient region. For the lower density case, they have a pronounced peaking close to the separatrix. This is further to be investigated.

The profile ECE system at ASDEX Upgrade allows for comparing the fluctuation levels across the entire plasma radius. Channels in the core and edge measure oscillations at the frequency of the quasi-coherent mode. Maximum mode amplitudes from the core and edge ECE measurements match the location of the steepest T_e gradient. The ECE instrument also enables phase measurements between the edge and core. With a steep gradient, the edge-core channels are anti-phase.

We challenge the refraction hypothesis by modeling the EC radiation transport with strong density and temperature perturbation at the edge, using 2D profiles. In the steep gradient phase, the core/edge behavior reproduces the experiment and the two channels are in anti-phase. The flat gradient case has in-phase behavior which correlates with the sign of the Te gradient in the core. The difference between the core and edge in the experiment is about a factor of five, while in the modeling, factor 100 is found.

Possible sources for the increased levels in the experiment are (i) The quasi-coherent mode potentially has a higher amplitude and broader radial extent at the edge than the JOREK small ELM case used as input. (ii) The ECE LOS for the modeled case was vertically closer to the axis, leading to a more perpendicular incidence angle and hence less temperature variation with the vertical refraction. (iii) The plasma potentially exhibits a rigid radial oscillation with the QCM frequency due to the strong variation of plasma pressure. So far, this work is showing that the refractive effects could play a role in the formation of the core ECE mode's signature. However, to further test this hypothesis, an extension of the work presented here is needed. Therefore, scans in the shape of the temperature profile and the amplitude of the density perturbation are planned for future work.

Acknowledgment

The author thanks Andres Cathey for providing JOREK data for input to the forward modeling. This work is supported by the US DOE under Award DE-SC0014264. This work has been carried out within the framework of the EUROfusion Consortium, funded by the European Union via the Euratom Research and Training Programme (Grant Agreement No 101052200 - EUROfusion). Views and opinions expressed are however those of the author(s) only and do not necessarily reflect those of the European Union or the European Commission. Neither the European Union nor the European Commission can be held responsible for them.

References

[1] M. Greenwald, R. Boivin, P. Bonoli, R. Budny, C. Fiore, J. Goetz, R. Granetz, A. Hubbard, I. Hutchinson, J. Irby et al., Physics of Plasmas **6**, 1943 (1999), https://doi.org/10.1063/1.873451

[2] L. Gil, C. Silva, T. Happel, G. Birkenmeier, G. Conway, L. Guimarais, A. Kallenbach, T. Pütterich, J. Santos, P. Schneider et al., Nuclear Fusion **60**, 054003 (2020)

[3] R. McDermott, C. Angioni, G. Conway, R. Dux, E. Fable, R. Fischer, T. Pütterich, F. Ryter, E.V. and, Nuclear Fusion **54**, 043009 (2014)

[4] A. Kallenbach, M. Bernert, P. David, M.G. Dunne, R. Dux, E. Fable, R. Fischer, L. Gil, T. Görler, F. Janky et al., Nuclear Fusion **61**, 016002 (2020)

[5] A.J. Creely, S.J. Freethy, W.M. Burke, G.D. Conway, R. Leccacorvi, W.C. Parkin, D.R. Terry, A.E. White,

Review of Scientific Instruments **89**, 053503 (2018), https://doi.org/10.1063/1.5005507

[6] S. Denk, R. Fischer, E. Poli, O. Maj, S. Nielsen, J. Rasmussen, M. Stejner, M. Willensdorfer, Computer Physics Communications **253**, 107175 (2020)

[7] Vanovac, B., Denk, S.S., Wolfrum, E., Willensdorfer, M., Suttrop, W., Fischer, R., Luhmann, N.C., ASDEX Upgrade Team, EPJ Web Conf. **203**, 02011 (2019)

[8] A. Cathey, M. Hoelzl, G. Harrer, M.G. Dunne, G.T.A. Huijsmans, K. Lackner, S.J.P. Pamela, E. Wolfrum, S. Günter, Plasma Physics and Controlled Fusion **64**, 054011 (2022)